New Journal of Physics
The open–access journal for physics

Inhomogeneous vortex distribution and magnetic coupling in oxide superconductor–ferromagnet hybrids

J Albrecht[1,2,4], M Djupmyr[1], S Soltan[3], H-U Habermeier[3], M R Connolly[2] and S J Bending[2]

[1] MPI für Metallforschung, Heisenberg strasse 3, D-70569 Stuttgart, Germany
[2] Department of Physics, University of Bath, Bath BA2 7AY, UK
[3] MPI für Festkörperforschung, Heisenbergstr. 1, D-70569 Stuttgart, Germany
E-mail: ja@mf.mpg.de

New Journal of Physics **9** (2007) 379
Received 18 July 2007
Published 22 October 2007
Online at http://www.njp.org/
doi:10.1088/1367-2630/9/10/379

Abstract. Hybrid systems of thin films of oxide ferromagnets and high-temperature superconductors have been investigated by scanning Hall probe microscopy (SHPM) to analyze the local magnetic flux density distribution at low temperatures. In addition to the intrinsic properties of the films themselves, such structures exhibit novel phenomena due to complex interactions arising at the interface between them. The latter can be divided into processes originating from either electronic or magnetic coupling, respectively. As a direct consequence, the distribution of vortices in the superconductor is strongly influenced by the magnetic background arising from the ferromagnet. The local magnetic information obtained from SHPM images provides clear evidence for the presence of a magnetic dipolar interaction between the magnetic domains of the ferromagnetic component and the vortex ensemble in the superconductor.

Superconductivity and ferromagnetism are generally incompatible phenomena and their combination in hybrid structures leads to substantial competition between the two ordering phenomena at interfaces between them [1]. In the case of hybrids of high-temperature superconducting $YBa_2Cu_3O_{7-\delta}$ (YBCO) and ferromagnetic $La_{2/3}Ca_{1/3}MnO_3$ (LCMO), this

[4] Author to whom any correspondence should be addressed.

PII: S1367-2630(07)55378-4

generally leads to the suppression of both transition temperatures [2, 3]. Several processes have been discussed to explain this observation, including oxygen diffusion [4] and charge transfer [5] due to a discontinuity in the chemical potential, a redistribution of the orbital occupancy [6], diffusion of spin-polarized quasiparticles [3, 7], and finally dipolar magnetic coupling via stray fields. Whereas the first three effects are limited to distances of a few nanometres around the interface, spin polarized quasiparticles and stray fields can have an influence on length scales of 100 nm and larger [8]. For appropriately designed geometries hybrid structures can be fabricated which benefit from the strong coupling between its components. For example, one can realize YBCO/LCMO hybrid structures that exhibit substantial magnetic pinning of flux lines in the superconductor, leading to asymmetric magnetic hysteresis loops [9, 10]. This magnetic flux line pinning is highly attractive for applications because it presents the possibility to control superconducting critical currents via external parameters. In contrast to heterostructures consisting of simple metals, magnetic pinning in oxide systems can be pronounced in the whole superconducting temperature range, not only close to the transition temperature [11]. This is directly related to the high-quality interfaces of these epitaxial multilayers [12]. It has been shown that magnetic pinning can also be present if both materials are *electronically* decoupled leading to the conclusion that the effect occurs due to *magnetic* interactions between ferromagnet and superconductor [10].

In this paper, we show for the first time spatially-resolved measurements of the local interaction between magnetic domain patterns in a ferromagnetic LCMO layer and flux line distributions in an adjacent YBCO layer. It is found that the stray magnetic fields due to the ferromagnet induce spontaneous vortices in the superconducting film. As a consequence a flux-free Meissner state is not observed after zero-field cooling. If an external magnetic field is now applied to this state, there are strong interactions between this spontaneous magnetic 'template' and additional flux lines penetrating into the superconductor. This is the first direct evidence for magnetic coupling between the magnetic domain pattern formed in the ferromagnetic LCMO and the flux lines penetrating the superconducting YBCO. At the same time the distribution of flux lines in the superconducting film is found to be highly inhomogeneous. This non-uniform vortex distribution leads, in turn, to modifications in the distribution of supercurrent density which will be discussed in more detail elsewhere [13].

Bilayers of LCMO and optimally doped YBCO have been prepared by pulsed laser deposition on single-crystal $SrTiO_3$ (STO) substrates. This allows the production of high-quality bilayers with atomically flat interfaces [12]. The individual thicknesses of the components typically lie in the range of 50–150 nm and, in the sample studied here, the superconducting layer was grown on top. This has important consequences. Firstly, the superconducting layer is much thinner than the *c*-axis penetration depth $\lambda_c > 1000$ nm allowing magnetic fields parallel to the film to readily penetrate the superconductor. Secondly, the preferred magnetization direction of the ferromagnetic LCMO films (grown on STO under tensile strain) is oriented in the plane of the film [14]. As a consequence Néel-type walls are formed between magnetic domains with an out-of-plane magnetization component.

The magnetic structures in these hybrids have been analyzed by scanning Hall probe microscopy (SHPM). Our microscope consists of a micron-sized Hall cross fabricated from a GaAs/AlGaAs semiconductor heterostructure containing a two-dimensional electron gas with high carrier mobility at low temperatures. This Hall cross is scanned over the sample at a fixed height of a few hundred nanometres and the Hall voltage recorded at each pixel of the image formed [15]. In the images presented here five consecutive images of the local magnetic

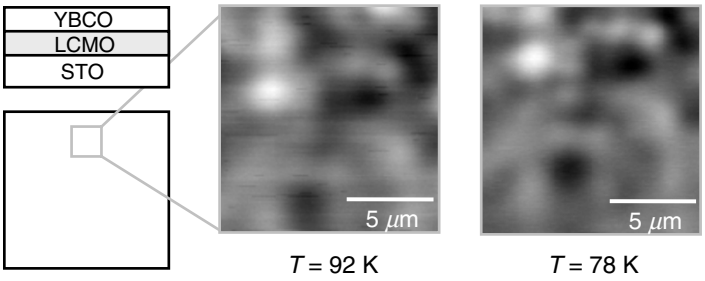

Figure 1. Sketch of the sample (left) and maps of the magnetic induction above the sample at temperatures above and below the superconducting transition. The grayscale spans −2.5 to 2.5 G. After accounting for a small shift of the measurement area as the temperature is reduced, very similar magnetic structures are observed in both images.

induction have been averaged to improve the signal-to-noise ratio. In this way, we are able to image the magnetic flux density distribution with a spatial resolution of better than 1 μm and a minimum detectable field of less than 10^{-2} G.

Figure 1 depicts a sketch of our sample geometry alongside two Hall probe images of a $13 \times 13\,\mu\text{m}^2$ square-shaped section of the film measured on a sample consisting of a 50 nm thick LCMO layer and a 100 nm thick YBCO layer. The measurements have been performed after zero-field cooling from room temperature to $T = 92$ K (left image) and afterwards to $T = 78$ K (right image). These temperatures are above and below the superconducting transition temperature of the sample, $T_c = 88$ K. The grayscale represents the perpendicular component of the local magnetic induction, where white (black) refers to positive (negative) values. This square-shaped area is located near the top edge of the sample as shown.

The two images depicted in figure 1 show almost identical magnetic flux density distributions. The only differences that can be seen arise from a slight shift in the scan region and a lower noise level at the lower temperature which is related to the carrier mobility of the Hall probe. No change in the observed magnetic pattern is found after crossing through the superconducting transition of the sample. This implies that the sample does not reach a flux-free Meissner state after passing into the superconducting state. Evidently, the adjacent ferromagnetic layer creates spontaneous vortices in the superconducting film. Since the LCMO layer has in-plane magnetization the magnetic stray fields will be predominantly parallel to the films. This flux is expected to readily penetrate into the YBCO layer since the relevant *c*-axis penetration depth ($\lambda_c = 1000$ nm) is much larger than the film thickness.

Figure 2 shows a line-scan across an SHPM image captured at $T = 78$ K after zero-field cooling. It has been extracted along the solid horizontal line superimposed on the image and characterizes neighboring areas of positive and negative flux, respectively, which are located in the top part of the image.

Since the ferromagnetic layer has in-plane anisotropy, regions of high out-of-plane magnetic field might be expected to relate to regions containing head-to-head domain walls. It is, however, likely that we measure the average flux of a domain structure which is much finer than can be resolved by our technique. The grayscale distribution in the image reveals that the local magnetic induction is highly inhomogeneous, with pronounced regions of opposing sign, even when mapped with a spatial resolution of about 1 μm. In practice, because of the small lateral

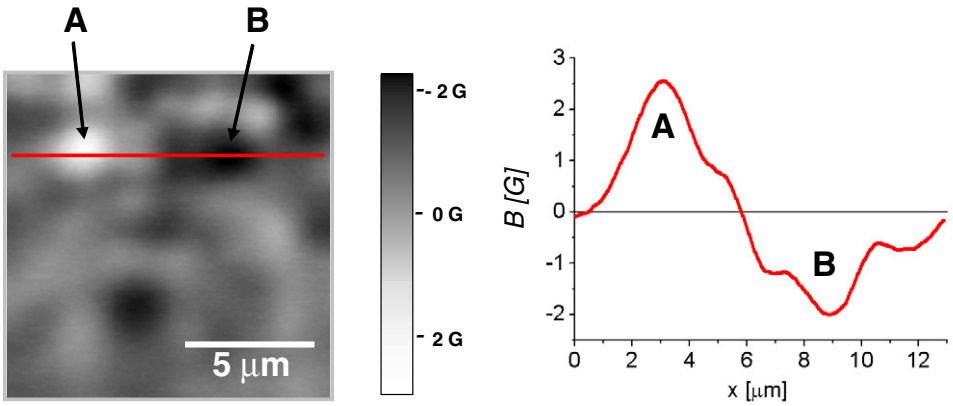

Figure 2. Left: SHPM image after zero-field cooling to a temperature of $T = 78$ K, the scale bar indicates the local magnetic induction. A and B mark two regions with out-of-plane oriented magnetic fields. Right: Line-scan of the magnetic induction across regions A and B along the solid horizontal line on the image.

dimensions of the domains, which are typically comparable to the film thickness of 50 nm, we cannot distinguish between contributions to our images from domains and domain walls. Hence, it is also possible that areas of strong contrast represent local regions of the LCMO film where the magnetization direction is out-of-plane. The question whether the domain structure of a single LCMO layer is modified due to the presence of the YBCO cap layer is a very interesting one, but far beyond the scope of this work. Here, we focus on the complete transfer of the magnetic structure from ferromagnet to superconductor, and its influence on the distribution of vortices. Since the 'magnetic' size of a vortex in YBCO thin films can easily exceed 1 μm [16], our Hall probe data directly access the length scales which are important for possible magnetic dipolar interactions.

Starting from the magnetic flux density distribution depicted in figure 2, a positive external field has been applied perpendicular to the film plane. A sequence of images of the same region of the sample at different external magnetic fields of 0.0, 3.3, 4.4, 5.1 and 5.9 Oe is shown in figure 3.

The sequence of images illustrated in figure 3 show that the magnetic pattern imposed by the manganite is unchanged at low fields. As the external field is increased above 4.4 Oe flux penetration can be recognized by the brightening of regions of the image. This corresponds to the magnetic signal due to flux lines penetrating into the superconducting component of the bilayer. It is not surprising that the LCMO magnetic template remains unaltered when the YBCO film enters the superconducting state since the exchange energy in the magnetic system is at least two orders of magnitude larger than the superconducting energy gap. However, it is certainly remarkable that the magnetic structure of the template also survives when vortices penetrate into the observed area.

To obtain more detailed information on the distribution of these vortices, figure 4 shows difference images at external applied fields of 4.4, 5.1 and 11.0 Oe. Here, the image of local magnetic induction at 3.3 Oe (reproduced on the left-hand side of figure 4) has been subtracted from the images at higher fields.

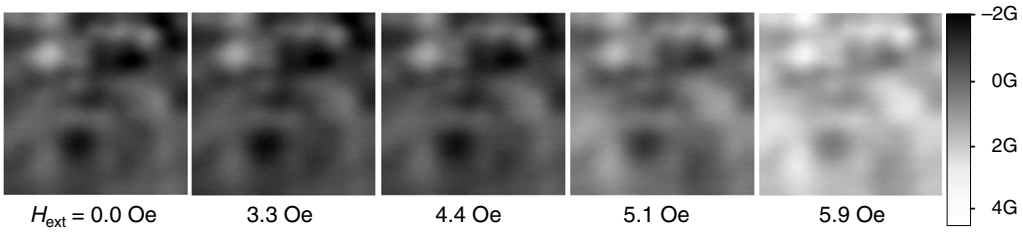

Figure 3. SHPM images of the area shown in figure 2 in increasing positive external magnetic fields. The penetration of magnetic flux into the sample is visible as brightening of the images starting from $H_{ext} = 4.4$ Oe onwards. Owing to our measurement geometry all magnetic flux lines have to penetrate from the top edge of the image which is closest to the physical edge of the sample.

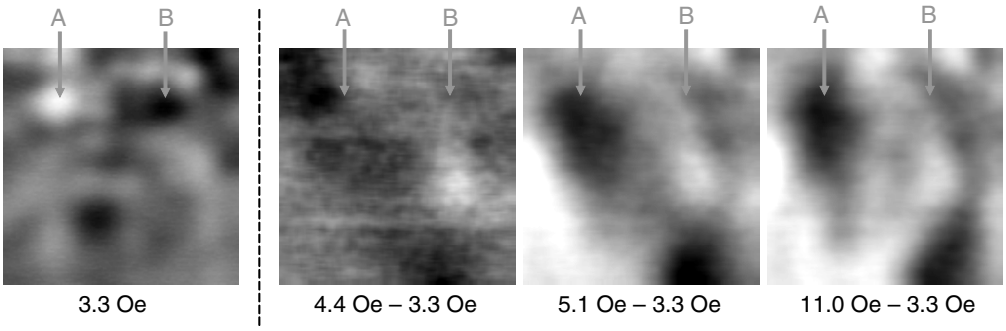

Figure 4. Difference images generated from the data of figure 3. The image at $H_{ex} = 3.3$ Oe has been subtracted from the images at higher fields to highlight the changes due to flux penetration into the superconductor. All images are optimized to maximum contrast.

Evidently large variations of the local flux density occur in the difference images depicted in figure 4, suggesting that the spatial distribution of penetrated vortices is also highly inhomogeneous (the local variations are larger than 1 G). In addition, the spatial size of the regions of high flux density is much coarser than that of the magnetic domain structures in the underlying ferromagnetic film.

For a full understanding of the images it is important to know the probable direction of motion of penetrating vortices. The field of view is located near the top edge of the sample resulting in a predominant flux penetration from the top (closest to the edge of the sample) downwards [17]. Hence, if we assume that the direction of flux motion is from top to bottom, we can now interpret the difference images of figure 4.

The most dominant feature of the first difference image at 4.4 Oe is a white, circular shaped area in the right part of the image. The image has been captured at the very initial stages of flux penetration. It can be seen that the first magnetic flux lines (the amount of flux corresponds to $2–3\Phi_0$, where Φ_0 denotes the magnetic flux quantum) have penetrated from the top exactly across the black area, which has been indicated with the label B. This indicates that this path

has to be a very easy one for the flux line motion. If we now further increase the external field to 5.1 Oe, we find the situation depicted in the next difference image. A large number of vortices (∼20–30) have penetrated into the imaged region, i.e. the macroscopic magnetic flux front has passed through it. Even now, the flux density remains highly inhomogeneous with large variations over a length scale of a couple of micrometres. Most of the image has now become white due to the increase in local flux density arising from the penetrated vortices. Just below the spot marked A, where the local magnetic induction was positive and oriented out-of-plane at the beginning of the experiment, a black shadow region is found. This 'shadow' region grows in size at higher external fields, for example the one depicted at $H_{ex} = 11.0$ Oe. This suggests that the path across the region of out-of-plane magnetic induction, which has the same orientation as the penetrating vortices, acts as an obstacle for vortex motion. The area behind the region marked A cannot be reached by vortices entering from the top of the field of view.

Our results can be described by a dipolar interaction between vortices and objects with out-of-plane magnetization (e.g. head-to-head domain walls or regions of local out-of-plane magnetization). If we have an antiparallel orientation of the fluxes in the local ferromagnetic area and the vortex, an attractive magnetic force is present which is able to describe the experimental finding that the first vortices that reach the investigated region penetrate across the region marked B. After this initial penetration of vortices the flux front arrives and flux lines penetrate all over the scan area except for ferromagnetic regions whose stray fields are parallel to those of the penetrating vortices (e.g. region A). Parallel orientation of the local ferromagnetic and vortex fluxes results in a repulsive dipolar interaction which prevents the magnetic flux lines from passing through region A. This directly leads to the black, shadow-like area which can be seen below region A in the two right hand images of figure 4. It is perhaps possible that the easy passage of the flux lines across area B could be related to the presence of a macroscopic defect in the superconductor which suppresses superconductivity locally and enhances flux penetration. However, the inhibition of flux line movement across the region A must be related to vortex repulsion due to interaction with spontaneous flux arising from and pinned by the magnetic structure of the ferromagnet. It is important to note, that all these processes take place in a strong pinning background provided by the defect structure of the YBCO film. This does not allow the observation of individual vortex pinning at magnetic sites, only the diversion of vortex motion due to anti-pinning sites can be seen.

These results clearly prove that there is a strong local magnetic interaction between the ferromagnetic domain pattern and the superconducting flux line ensemble in oxide ferromagnet-superconductor hybrids. The fact that this interaction only weakly influences the critical current density of the YBCO film is due to the inhomogeneous distribution of spontaneous flux from magnetic domains that can act as barriers for vortex movement. As long as these regions do not form a continuous network throughout the film the flux lines always can find a percolation path which avoids them. The preparation of magnetic structures to optimize critical currents in these hybrid systems is a challenge for the future.

In conclusion, we have directly imaged the distribution of vortices penetrating into an oxide superconductor–ferromagnet hybrid structure. Our SHPM results clearly reveal a magnetic dipolar interaction between the magnetic domain pattern in the ferromagnet and penetrating superconducting vortices. This leads to an inhomogeneous distribution of vortices in the superconducting component of the hybrid structure. It is also clear why these magnetic interactions only have a very slight influence on the critical current density. The magnetic vortices in the superconductor are able to percolate around areas of parallel magnetic flux,

and hence always find an easy path to penetrate into the superconductor. Future work will focus on texturing the domain structure in the LCMO layer to eliminate these percolation paths. This would effectively inhibit flux line movement and increase flux line pinning and critical currents in such hybrid structures.

References

[1] Sá de Melo C A R 1997 *Phys. Rev. Lett.* **79** 1933
[2] Sefrioui Z, Arias D, Peña V, Villegas J E, Varela M, Prieto P, León C, Martinez J L and Santamaria J 2003 *Phys. Rev.* B **67** 214511
[3] Soltan S, Albrecht J and Habermeier H-U 2004 *Phys. Rev.* B **70** 144517
[4] Chakalov R A, Passerieux G, Jones I P, Mikheenko P, Ireland J, Chakalova R I, Colclough M S and Muirhead C M 2005 *J. Appl. Phys.* **98** 123908
[5] Varela M, Lupini A R, Pennycook S J, Sefrioui Z and Santamaria J 2003 *Solid-State Electron.* **47** 2245
[6] Chakhalian J *et al* 2006 *Nat. Phys.* **2** 244
[7] Habermeier H-U, Soltan S and Albrecht J 2007 *Physica* C **460** 32
[8] Soltan S, Albrecht J and Habermeier H-U 2007 *Mater. Sci. Eng.* B doi:10.1016/j.mseb.2007.07.081
[9] Przyslupski P, Komissarov I, Paszkowicz W, Dluzewski P, Minikayev R and Sawicki M 2004 *Phys. Rev.* B **69** 134428
[10] Albrecht J, Soltan S and Habermeier H-U 2005 *Phys. Rev.* B **72** 092502
[11] van Bael M J, Temst K, Moshchalkov V V and Bruynseraede I 1999 *Phys. Rev.* B **59** 16674
[12] Habermeier H-U, Cristiani G, Kremer R K, Lebedev O and Van Tendeloo G 2001 *Physica* C **364** 298
[13] Djupmyr M, Soltan S, Habermeier H-U and Albrecht J unpublished
[14] Kwon C *et al* 1997 *J. Magn. Magn. Mater.* **172** 229
[15] Oral A, Bending S J and Henini M 1996 *Appl. Phys. Lett.* **69** 1324
Oral A, Bending S J and Henini M 1996 *J. Vac. Sci. Technol.* B **14** 1202
[16] Pearl J 1964 *Appl. Phys. Lett.* **5** 65
[17] Jooss C, Albrecht J, Kuhn H, Leonhardt S and Kronmüller H 2002 *Rep. Prog. Phys.* **65** 651